AJNR

Analysis of Slipstream Flow in a Wide-necked Basilar Artery Aneurysm: Evaluation of Potential Treatment Regimens

Steven G. Imbesi and Charles W. Kerber

AJNR Am J Neuroradiol 2001, 22 (4) 721-724
http://www.ajnr.org/content/22/4/721

AJNR Am J Neuroradiol 22:721–724, April 2001

Technical Note

Analysis of Slipstream Flow in a Wide-necked Basilar Artery Aneurysm: Evaluation of Potential Treatment Regimens

Steven G. Imbesi and Charles W. Kerber

Summary: A replica of a lethal wide-necked basilar artery aneurysm was created by casting a deceased patient's brain vessels and then placing the replica in a circuit of pulsating optically clear non-Newtonian fluid. Individual fluid slipstreams were opacified with isobaric dyes, and images were recorded on film. Studies were completed on the vascular replica, then were repeated, first after placement of a stent across the aneurysm neck and then after placement of Guglielmi detachable coils into the aneurysm sac through the stent. The slipstreams entered the untreated aneurysm via the distal aneurysm neck (the inflow zone), impacting against the distal lateral aneurysm wall. When the stent was placed across the aneurysm neck, the slipstreams lost coherence and did not strike the aneurysm sidewall. Placing the coils further disturbed and reduced aneurysmal flow, especially when the coils filled the inflow zone at the distal lateral aneurysm sac.

Flow dynamics of the intracranial circulation and, in particular, of intracranial aneurysms have been previously studied and described using computer models and actual human vascular casts (1–3), although much remains unknown. A more comprehensive understanding of these dynamic principles and the perturbations that various treatment strategies induce in flowing blood should provide safer and more permanent aneurysm obliteration. We recently had the opportunity to make an in situ casting of the brain arteries of a patient who died of a ruptured intracranial basilar artery aneurysm, reproduced the aneurysm and surrounding arterial system, and studied the flow dynamics in the system before and after endovascular treatment. We report the results of those experiments.

Received July 12, 2000; accepted after revision September 26.

From the Departments of Radiology and Neurosurgery, Hospital of the University of Pennsylvania, Philadelphia (S.G.I.), and the Departments of Radiology and Neurosurgery, University of California, San Diego.

Presented at the annual meeting of the American Society of Neuroradiology, Atlanta, April 2000.

Address reprint requests to Steven G. Imbesi, MD, Assistant Professor of Radiology and Neurosurgery, Hospital of the University of Pennsylvania, 3400 Spruce St, Philadelphia, PA 19104.

Technique and Observations

A 58-year-old woman with subarachnoid hemorrhage had undergone angiographic evaluation, and while en route to the operating room, bled again and died. After obtaining consent for vessel infusion and harvest by the patient's family, we brought her back to the radiology department and infused the vertebral vascular system with epoxy. After recovering the brain and associated vessels during the autopsy, we created a mold of the arteries and aneurysm using the lost-wax technique. Details of this process have been described previously (4).

Two clear elastic silicone replicas were made from the original casting. The replicas were placed in a circuit of pulsatile non-Newtonian fluid that mimics the rheologic properties of blood (5). A blood pump (model 1421, Harvard Apparatus Corp, S Natick, MA) cycling at one pulse per second provided fluid flow. Flows were adjusted to replicate human physiological flow profiles with a Square Wave electromagnetic flowmeter (Carolina Medical Electronics, King, NC), so that there was 40% forward flow during diastole as compared with flow during systole. Polyvinyl alcohol particles were placed in the flowing fluid and the distance they traveled over time was measured to calculate flow velocity. We standardized the basilar artery flow volume at 200 mL/min (0.003 L/s) and peak systolic velocity at 80 cm/s (0.8 m/s), similar to that found in healthy humans. The fluid slipstreams were opacified with isobaric dyes after an insertion of 30-gauge needles into the vessel sidewall. Images were recorded on 35-mm film at shutter speeds up to 1/1000 of a second and on Super VHS digital video at shutter speeds up to 1/30 of a second. Images were obtained of the flow dynamics in the untreated vascular replica, then with the same flow parameters verified by the electromagnetic flowmeter, after placement of a 4.5 × 20-mm coronary stent (Magic Wallstent, Boston Scientific, Natick, MA) across the aneurysm neck, and then after placement of the Guglielmi detachable coils into two different parts of the aneurysm sac: the distal portion (the inflow zone) and the proximal portion. Five observations were made for each of the three vascular conditions, all of which were compared. Since flow in the anterior inferior cerebellar arteries was not germane to the current aneurysmal flow analysis, these vessels were not replicated in the pretreatment model and, for consistency, were tied off in the model used for the posttreatment experiment.

In the untreated basilar artery aneurysm system, undisturbed fluid slipstreams came together at the vertebral artery confluence, passed distally along the greater curvature, and entered the distal portion of the center of the aneurysm neck via a relatively small inflow zone, directed there by the curved parent artery and the aneurysm origin acting as a flow divider. Those high-energy pulsatile slipstreams impacted against the distal lateral aneurysm wall, the point at which it had ruptured. The slipstreams and also the particles (not shown in this article), once having struck the point of rupture, would then swirl around the periphery of the aneurysm, initially posterolaterally, then medially, in a relatively slow-moving helically flowing central zone, finally passing rapidly out the aneurysm neck

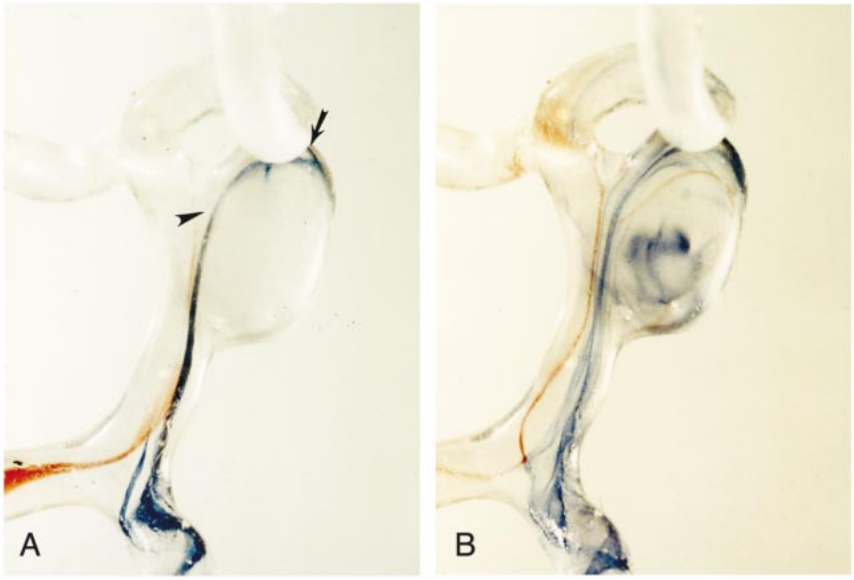

FIG 1. The wide-necked basilar artery aneurysm replica.

A, At peak systole (defined as peak flow within the basilar artery), opacified fluid slipstreams enter the aneurysm sac through the distal neck (*arrowhead*) and impact the distal lateral aneurysm wall (*arrow*), the site of aneurysm rupture.

B, Flow swirls within the aneurysm sac and exits the aneurysm neck (during the next systole) peripheral to the distal central incoming jet, usually at the proximal portion of the neck. As flow is not compressible, maximal flow is during systole.

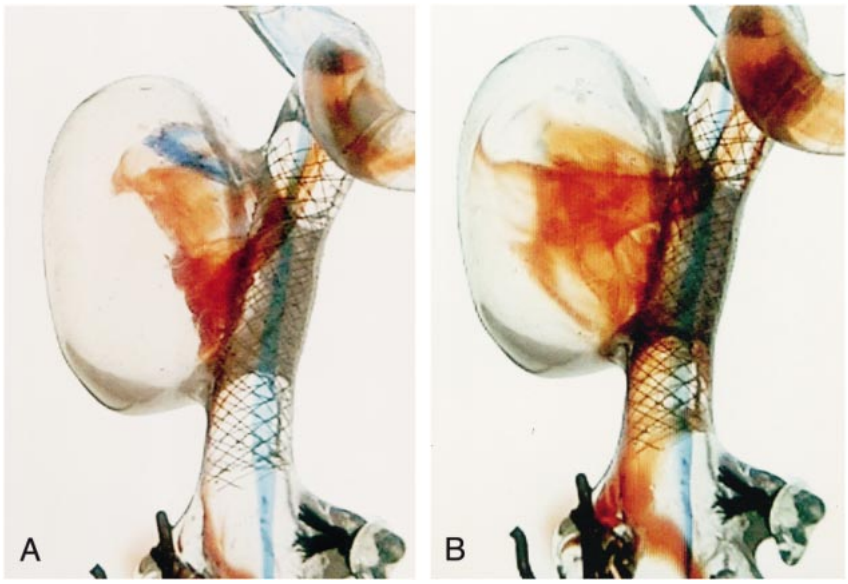

FIG 2. Wide-necked basilar artery aneurysm after treatment with parent vessel stenting.

A, Fluid slipstreams lose coherence as they pass through the stent mesh with little if any impact against the aneurysm sidewall.

B, Flowing slipstreams generally remain within the center of the aneurysm sac and the intraaneurysmal reverse vortex flow pattern previously shown has changed to a more disturbed flow profile.

circumferentially about the inflow zone during the next systole (Fig 1). The flow was similar during diastole, but less vigorous.

After the stent was placed across the aneurysm neck, the slipstreams changed dramatically. Those slipstreams that did enter the aneurysm sac lost their coherence and, as they passed through the stent mesh, diffused generally into the center of the aneurysm. Rapid flow into the aneurysm appeared to decrease significantly, and the previously seen violent slipstreams impacting against the distal aneurysm wall were no longer visible. None of the previously seen flow pattern remained (Fig 2).

When coils were placed into the aneurysm sac via a microcatheter directed through the stent mesh, distally placed coils further prevented inflow of slipstreams into the impact zone, the point of rupture. Even though the coils were packed loosely, there was great disturbance of flow, with slowing of the slipstreams generally throughout the aneurysm and in the interstices of the coil mass. When the coils were placed proximally, no significant difference in flow dynamics was evident, as compared with that seen with the stent placement alone (Fig 3). As more coils were placed in an attempt to achieve more complete coil compaction, they began to deform the stent and narrow the parent vessel lumen, because of the extremely wide aneurysm neck and the aneurysm's large size.

Discussion

In the last decade, there has been a greater appreciation for the need to understand flow dynamics in large vessels, especially the cranial vasculature, if good long-term treatment results are to be obtained. Modeling of the cerebral vasculature is a difficult process, and when 3D analysis is introduced, tremendous computer power is required. Our approach has been to directly cast human vessels, making high-fidelity anthropomorphic vascular replicas, and then to place those replicas in circuits of fluid with the flow dynamics matched as closely as possible to those found in humans. Careful adjustment of the system is necessary to repli-

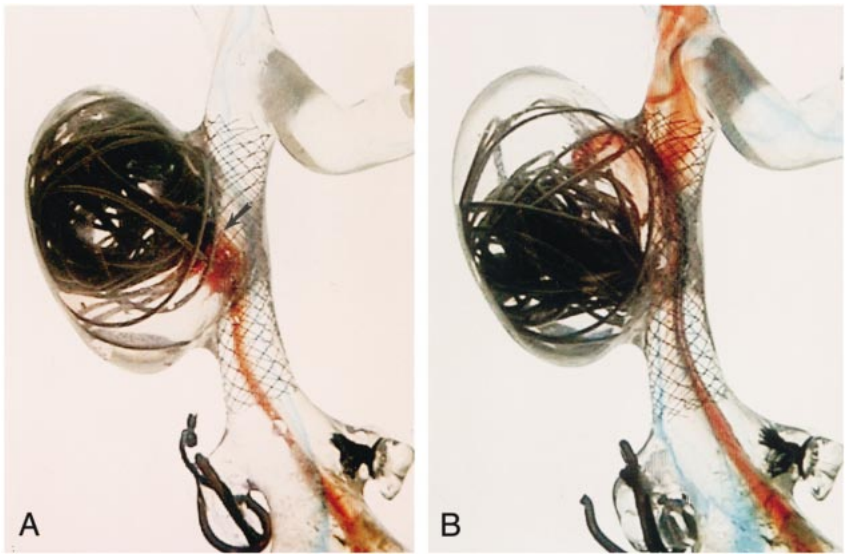

FIG 3. Wide-necked basilar artery aneurysm after treatment with parent vessel stenting and subsequent intraaneurysmal coiling.

A, Coil placement in the distal lateral aneurysm segment results in slipstream impact against the coil mass (*arrow*) with little flow entering the aneurysm and with no slipstream impact against any portion of the aneurysm sidewall.

B, Coil placement in the proximal lateral aneurysm segment results in some flow entering the aneurysm; however, the stent continues to interrupt the coherence of the entering fluid slipstreams.

cate the pulsatile flow found in human vessels, and our system corresponds to the flow profiles found at Doppler sonography (6). In this case, the value of the system is evident when direct visualization of the slipstream shows its impact on the aneurysmal rupture site, suggesting flow similar to that which occurred in the patient from whom the replica was harvested. Evaluation and understanding of the vascular flow helps elucidate the pathophysiology of the disease process (3). Alteration of these abnormal slipstreams via endovascular devices may result in innovative therapies for disease treatment, as demonstrated by this experiment.

Presently, endovascular treatment of wide-necked aneurysms is quite limited. The coils tend to migrate from the aneurysm sac into the parent vessel, despite placement of a balloon adjacent to the aneurysm neck, described first by Guglielmi and colleagues (7) and later by Moret et al (8). A second potential technique would be to cross the vessel neck with a stent. Stent placement is presently limited by the difficulty in traversing the bends in the carotid and vertebral arteries where those vessels enter the skull, but already, clinical success has been achieved by this technique (9, 10).

Our result in placing a mesh stent across the aneurysm neck, which dramatically decreased the violence of the slipstreams impacting the aneurysm, corroborates the findings in an excellent series of studies of side-wall aneurysm models, in which the authors' observations parallel our own (11, 12). The placement of stents across the aneurysm orifice of both replicas and models significantly altered the inflow characteristics, and most particularly, the powerful central slipstreams that strike at the dome. Whether a simple placement of a stent across an aneurysm orifice will disturb the flow enough to induce thrombosis remains to be seen clinically.

If it is thought that the stent has not altered the flow sufficiently to promote permanent thrombosis, it is possible to insert a microcatheter through the stent mesh and into the aneurysm sac. Our findings suggest that those coils should be placed at the aneurysm inflow zone. While incomplete packing of coils within the aneurysm sac may theoretically displace the inflow zone and subsequently the impact site to a different part of the aneurysm, our observations show that the inflowing slipstreams directly impact the coil mass (when coils are placed in the distal lateral aneurysm segment) and do not create new regions of aneurysm inflow. Additionally, one might assume that the impact force is now distributed over a greater surface area of the aneurysm sac (the surface area of the coil mass) as opposed to the pretreatment direct point of impact. These observations support the assertion that this partial treatment algorithm should reduce the risk of aneurysm rupture.

Conclusion

The creation of replicas of human vascular abnormalities, particularly aneurysms, is a tedious and technically difficult undertaking, but should allow a more complete and deeper understanding of the vascular flow dynamics that led to the abnormality in the first place. As important, such replicas should further an understanding of vascular abnormalities that permits the design of better treatment paradigms for these often lethal diseases.

References

1. Kerber CW, Heilman CB. **Flow dynamics in the human carotid artery.** *AJNR Am J Neuroradiol* 1992;13:173–180
2. Burleson AC, Strother CM, Turitto VT. **Computer modeling of intracranial saccular and lateral aneurysms for the study of their hemodynamics.** *Neurosurgery* 1995;37:774–782

3. Imbesi SG, Kerber CW. **Analysis of slipstream flow in two ruptured intracranial cerebral aneurysms.** *AJNR Am J Neuroradiol* 1999;20:1703–1705
4. Kerber CW, Heilman CB, Zanetti PH. **Transparent elastic arterial models, I: a brief technical note.** *Biorheology* 1989;26: 1041–1049
5. Mann DE, Tarbell JM. **Flow of non-Newtonian blood analog fluids in rigid curved and straight artery models.** *Biorheology* 1990;27:711–733
6. Keller HM, Merer WE, Anliker M, et al. **Non-invasive measurement of velocity profiles and blood flow in the common carotid artery by pulsed Doppler ultrasound.** *Stroke* 1976;7:370–377
7. Giglielmi G, Vinuela F, Briganti F, Duckwiler G. **Carotid-cavernous fistula caused by a ruptured intracavernous aneurysm: endovascular treatment by electrothrombosis with detachable coils.** *Neurosurgery* 1992;31:591–597
8. Moret J, Cognard C, Weil A, Castaings L, Rey A. **Reconstruction technic in the treatment of wide-necked intracranial aneurysms: long-term angiographic and clinical results: apropos of 56 cases.** *J Neuroradiol* 1997;24:30–44
9. Wilms G, van Calenbergh F, Stockx L, Demaerel P, van Loon J, Goffin J. **Endovascular treatment of a ruptured paraclinoid aneurysm of the carotid siphon achieved using endovascular stent and endosaccular coil placement.** *AJNR Am J Neuroradiol* 2000;21:753–756
10. Sekhon LHS, Morgan MK, Sorby W, Grinnell V. **Combined endovascular stent implantation and endosaccular coil placement for the treatment of a wide-necked vertebral artery aneurysm: technical case report.** *Neurosurgery* 1998;43:385–388
11. Aenis M, Stancampiano AP, Wakhloo AK, Lieber BB. **Modeling of flow in a straight stented and non-stented side wall aneurysm model.** *J Biomech Eng* 1997;119:206–212
12. Lanzino G, Wakhloo AK, Fessler RD, Hartney ML, Guterman LR, Hopkins LN. **Efficacy and current limitations of intravascular stents for intracranial internal carotid, vertebral, and basilar artery aneurysms.** *J Neurosurg* 1999;91:539–547